AIAA 99-1042

Measurements of the Progress-M Main Engine Retrofiring Plume at Orbital Conditions

G. F. Karabadzhak, Yu. Plastinin, A. Afanasiev, and
E. Szhenov
TsNIIMASH, Korolev, Russia

J. A. Drakes, W. K. McGregor, J. A. Nichols, and
R. A. Reed
Sverdrup Technology, Inc., AEDC Group
Arnold Engineering Development Center
Arnold Air Force Base, Tennessee 37389

D. Bradley
USAF, Arnold AFB, TN

V. Teslenko, N. Shvets, O. Volkov, and V. Kukushkin
RSC Energia, Korolev, Russia

37th AIAA Aerospace Sciences Meeting & Exhibit
January 11-14, 1999 / Reno, NV

AIAA-99-1042

Measurements of the Progress-M Main Engine Retrofiring Plume at Orbital Conditions*

*G. F. Karabadzhak,† Yu. Plastinin,† A. Afanasiev,‡ E. Szhenov,‡ J. A. Drakes,** W. K. McGregor,†† J. A. Nichols,‡‡ R. A. Reed,‡‡ D. Bradley,*** V. Teslenko,††† N. Shvets,††† O. Volkov,††† and V. Kukushkin†††*

Abstract

An experiment set has been performed using the Progress-M spacecraft and a set of dedicated and non-dedicated maneuvers in the vicinity of the Mir space station. The purpose of the experiment was to acquire ultraviolet data from the far-field glow of rocket exhaust plumes at very high altitudes. Ultraviolet imagery of the Progress main engine was acquired using a camera with a response function that peaked at 290 nm. The data show an intense near-field radiation accompanied by a low-level glow that exists over spatial scales of kilometers. The emission is attributed to the decay of the OH(A) state, presumably formed in reactive collisions of plume species with atmospheric atomic oxygen. While many observations were recorded of the main engine that is used on both the Progress-M and Soyuz-TM spacecraft, as well as the smaller attitude control system thrusters, two key main engine measurements are reported here. In the first measurement, the imager field of view was at a right angle to the plume axis, at a radial range of 9.2 km. The firing lasted 5.3 sec. In the second measurement of the main engine plume, the aspect angle varied from 173 to 168 deg while the range from the main engine to the Mir station ranged from 15 to 28 km. The firing lasted 244 sec in that case. In both measurements, the far-field emission was found to completely fill the imager field of view. A relatively sluggish rise of the far-field radiation was observed at ignition, as compared to the near-field radiation. The measurements of the far-field plume were calibrated using the irradiance of a known star. It was estimated that within the portion of the plume observed by the imager, the plume radiated 30 and 180 W of power for the first and second measurements, respectively. These results are briefly compared with the requirements for OH(A) generation from the H_2O + O reaction.

Introduction

The issues surrounding the radiation emitted during the operation of a spacecraft thruster in low Earth orbit have been investigated for decades, depending upon the altitude regime and wavelengths of interest. The radiation has its origin in a wide range of physical processes ranging from combustion of unburned propellants to atmospheric heating of the jet flow. This work concerns itself with one aspect of the radiation from exoatmospheric plume jet flows typical for operations of orbiting craft such as the U. S. Shuttle, the space station Mir, or the International Space Station. At these altitudes, ranging from 250 km to 400 km, the atmosphere is extremely rarefied, with the ambient density varying from 10^9 to 10^8 molecule-cm^{-3}, respectively. Not only is the atmosphere very thin, but its composition is also mostly atomic oxygen, leading to the possibility of reactions between the ambient environment and the combustion gases expelled from the spacecraft thrusters.

---

* The research reported herein was performed by the Arnold Engineering Development Center (AEDC), Air Force Materiel Command. Work and analysis for this research were performed by personnel of Sverdrup Technology, Inc., AEDC Group, technical services contractor for AEDC. Further reproduction is authorized to satisfy needs of the U. S. Government.

† TsNIIMASH, Korolev, Russia, Member, AIAA.

‡ TsNIIMASH, Korolev, Russia.

** Sverdrup Technology, Inc., Arnold AFB, TN, Senior Member, AIAA.

†† Sverdrup Technology, Inc., Arnold AFB, TN, Associate Fellow, AIAA.

‡‡ Sverdrup Technology, Inc., Arnold AFB, TN.

*** USAF, Arnold AFB, TN

††† RSC Energia, Korolev, Russia

The present work reports on a study of the ultraviolet emission detected from the jet flow of a Russian Progress-M cargo spacecraft main engine. The identical engine is also used in the Soyuz-TM crew transfer vehicle, which is a derivative of the Progress-M. Cosmonauts aboard Mir first detected the radiation in 1993, using a filtered ultraviolet imager with a bandpass encompassing the OH(A-X) electronic band emission wavelength of 306 nm. Since that time, numerous improvements in the imager technology have been incorporated, providing enhanced spatial resolution and sensitivity. Based upon the first opportunistic observations in 1993, an organized effort was undertaken in the winter of 1996, known in the U. S. as MirEx and in Russia as RELAXATION to systematically study, among other things, the radiation detected by the ultraviolet imager. This radiation is believed to be predominantly OH(A-X). This effort began with a complete review of the available radiometric instrumentation aboard the Mir station. Three instruments were chosen for use in the ultraviolet plume study: the aforementioned UV imager, a VUV/UV spectrometer, and an IR spectrometer. Unfortunately, the 1997 accidental collision of a Progress-M with the Mir damaged the VUV/UV spectrometer as well as the positioning mechanism of the IR spectrometer. This problem was partially resolved, however, when a replacement instrument was sent to Mir in February 1998.

In addition to our work on Mir, there has been work done by other researchers to understand issues of jet flow radiation at high altitudes. In particular, the work by Viereck, et al.[1,2] in which the exhaust plumes from the U. S. Shuttle PRCS and VRCS thrusters were observed by instruments in the Shuttle bay, as well as the AMOS telescope facility in Maui. That work explored the visible region of the spectrum using both a bandpass imager and spectrometer as the Shuttle underwent dedicated ram and wake burns.

Subsequent work by the same group investigated the production of excited state NH in thruster exhaust plumes. This time, they employed the Shuttle PRCS and VRCS thrusters while observing the radiation from the AMOS facility, as well as the GLO camera in the Shuttle bay.

The data recorded by the GLO spectro-imager represent some very high quality near-field data from the thruster plumes. The GLO instrument is a composite of numerous sensors and had an effective bandpass from 110 nm to 1100 nm. The emission data were acquired during a series of PRCS and VRCS burns ranging from ram to wake in direction. The altitude of the Shuttle for the published data was 320 km. The PRCS thruster data, taken in a ram burn, show strong OH(A), NH(A), NO_2, and HNO in the exhaust 4 m from the nozzle exit, and strong OH(A), NH(A), and O(^{1}S) and O(^{1}D) line emission at 33 m downstream of the nozzle exit plane.

Given the general phenomenological understanding obtained from the visible and near-UV experiments above, a reasonable extension is that other observed plume emissions are also due to interactions of the plume with the atomic oxygen of the atmosphere. The availability of the instrumentation on Mir provided an excellent opportunity to investigate the next logical choice of plume emission, the OH(A-X) emission observed by both Viereck, et al. in 1996 as well as the Russian cosmonauts in 1993. The goal of the experiment was to determine if the OH emission was due to interactions between the plume and the atmosphere, as opposed to interactions among plume species. If this was found to be true, then a secondary objective of the experiment was to acquire sufficient data to be able to test a hypothesis for OH(A) generation previously put forth by the authors, namely $O + H_2O \rightarrow OH + OH(A)$.[3]

Apparatus

While numerous data collection events were performed under this experiment, this report will focus on two similar exercises involving the main engine for both the Progress-M and Soyuz-TM spacecraft, denoted here as the PME. Data were acquired on the PME using two instruments, a UV imager and a UV spectrometer.

The UV imager was developed and manufactured at TsNIIMASH in cooperation with the Optical Department of Lebedev's Physical Institute. It combines a quartz telescope followed by an image intensifier and relay lens to interface with a radia-

tion detector. To effectively block the visible radiation a solar blind Cs_2Te photocathode is used in the image intensifier. Also, the UV imager is equipped with a broadband color glass UV filter and three different narrow-band (8-nm HWHM) interference filters. Although the complete description is provided in Ref. 3, some general characteristics of the UV imager are given in Table 1.

Table 1. The UV Imager General Characteristics

Operating wavelength region, nm	200 – 360
Wide band color UV filter, nm	260 – 380
Interference filters center wavelength, nm	260, 285, 317
Telescope effective diameter, mm	55
Telescope focal length, mm	78
Maximum field of view, deg	12
Angular resolution, angular minutes	4.0
Image intensifier maximum gain	~ $3 \cdot 10^4$

The UV spectrometer is a small, portable device (Model S2000) manufactured by Ocean Optics Inc. of Florida and comprises the spectrometer itself, a 2-m-long fiberoptic cable, a 600-μm entrance aperture, and a focusing 5-mm-diam UV-grade lens. A Toshiba Satellite Notebook computer with a high-speed A/D card is used to control the spectrometer and the digital data acquisition. The general features of the spectrometer are listed in Table 2.

Table 2. UV Spectrometer Specifications (Ocean Optics Model S2000)

Wavelength region, nm	230-380
Number of channels	2048
Spectral resolution, nm (FWHM)	0.4
Minimum sampling time, sec per spectrum	0.02

In the application on Mir, the UV imager is mounted in the Mir interior onto a 3-axis gimbaling mount that attaches directly to the interior side of a Mir window port. The UV spectrometer fiber-optic focusing lens is rigidly fixed to the body of the UV imager, such that the imager and spectrometer are co-aligned. For the experiment set considered here, only the quartz windows on the Mir core module were used for plume observation.

The instruments are operated by the cosmonauts aboard Mir, with guidance from the ground. The image data on the intensifier screen are recorded by a standard video camera, using Beta-CamSP Professional videotapes. These tapes can be either transferred to Earth during a crew transfer mission, or played on Mir and telemetered down. Since telemetry can introduce noise into the video train, the preferred method is direct transfer of the data tapes. However, data tape delivery to Earth only occurs in conjunction with Mir station crew transfers, which are roughly every six months, making telemetry downlink of the image data a necessary step in order to perform timely analyses. The spectrometer data are digital and much less voluminous, and can be transferred via telemetry to the ground with virtually no data quality loss.

The data sets of interest here involve PME burns on May 15, 1998, and August 25, 1998. The PME motor propellants are UDMH and N_2O_4 at an O/F of 1.8. The nozzle area ratio is 48, providing a thrust of 3100 N. The predicted products of combustion are listed in Table 3.

Table 3. Predicted Combustion Products at the PME Exit Plane

Species	Mole Fraction
H_2O	0.2884
N_2	0.2668
H_2	0.1905
CO	0.1891
CO_2	0.0531
H	0.0110
O	1E-5
OH	1E-5

The combustion modeling is described in Ref. 3, while the exhaust flow modeling is described in more detail in Drakes, et al.[4] The identical motor is used for both the Progress-M and Soyuz-TM spacecraft.

Experiment Scheme

In the case of May 15, 1998, a dedicated maneuver by a dedocking Progress-M cargo ship was undertaken near the Mir station. Prior to dedocking, the Mir was oriented such that the Progress ship was attached to the forward position relative to the velocity vector, and the instrumentation was looking straight down to the dark Earth

below. The initial altitude of the Mir station-Progress-M combination was 390 km. Following the mechanical push-off of the Progress-M from Mir, the cargo ship rose above the Mir station and executed a short retrofiring, as shown schematically in Fig. 1. In this, the Mir is placed at the origin for reference and distances are measured relative to Mir. This first positioning burn sent the Progress into a trajectory that brought it behind and subsequently beneath the Mir to the point where the second positioning burn, dV2, was fired.

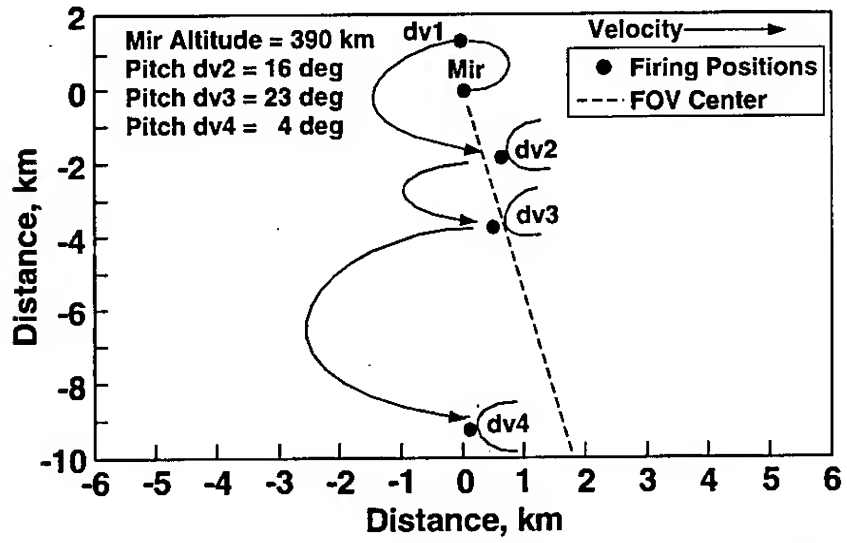

Figure 1. Trajectory for the May 15, 1998 Progress-M dedocking. All distances relative to Mir.

The center of the UV imager field of view (FOV) is shown in this figure as the dotted line. The velocity of the Mir and Progress-M was approximately 7.38 km/sec in the local horizontal direction. The PME pitch angle was fairly steep, roughly 23 deg, and no signal in the imager was detected. For clarity, the pitch angle of the PME is equivalent to the vehicle angle of attack in these experiments, since the velocity vector is always parallel, or nearly so, to the local horizon. The imager had an angular field of view of 5 deg, which at this range implies a footprint on the dV3 plume axis which covered from 50 to 350 m downstream of the nozzle exit. The final burn, dV4, occurred at 9.2 km from the Mir, and the center of the UV imager FOV was located downstream of the nozzle exit by ~1.6 km. The imager had an angular field of view of 5 deg, which means the imager footprint on the dV4 plume axis extended from roughly 1.2 km to 2.0 km downstream of the nozzle exit. The dV4 firing had a small pitch angle, and an emission signal was reliably detected in the UV imager.

Although the Progress-M dedocking itself must occur in daylight over ground telemetry stations, all three dedicated burns occurred in darkness, following the crossing of the terminator by the spacecraft.

The second experiment to be discussed in this report occurred on August 25, 1998. It was the Soyuz-TM main reentry burn. Since this was a manned craft, safety considerations limited the extent of maneuvering that could be done on our behalf, and the observation of the plume had to occur on an opportunistic basis only. Fortunately, the reentry burn occurred in darkness. The ballistics of the August 25, 1998 event are shown in Fig. 2.

First, it should be noted that the braking burn for reentry lasts for ~4 minutes. The procedure is to start by allowing the Soyuz-TM to fall into position 15 km behind the Mir, and at slightly higher altitude. Note the Soyuz is at 385 km at ignition and traveling at 7.35 km/sec velocity. During the time of the burn of the PME, the Soyuz-TM will move to an altitude of 377 km, with a pitch angle relative to the velocity vector of over 15 deg. The range to the Mir station will increase from 15 km to ~28 km. The viewing aspect for this reentry burn is also shown in Fig 2. At ignition, the aspect angle measured from the Soyuz velocity vector is roughly 7 deg, or 173 deg if measured from the nose of the craft. By the time shutdown occurs, the aspect angle measured from the nose has decreased to 168 deg.

The orientation of the Mir with the Soyuz-TM is essential to understanding the imagery presented below. Figure 3 attempts to illustrate the relative positions of the two spacecraft at motor ignition and motor shutdown. At ignition, the Soyuz-TM is behind and slightly higher than the Mir station. Thus, the instruments are looking up to the Soyuz-TM nozzle. Once the motor ignites, the Soyuz-TM velocity vector and plume thrust vector separate into different directions, as the motor is slowly braking the spacecraft. The aspect angle widens from 7 deg to 12 deg measured from the plume axis, or 173 deg to 168 deg measured from the craft nose.

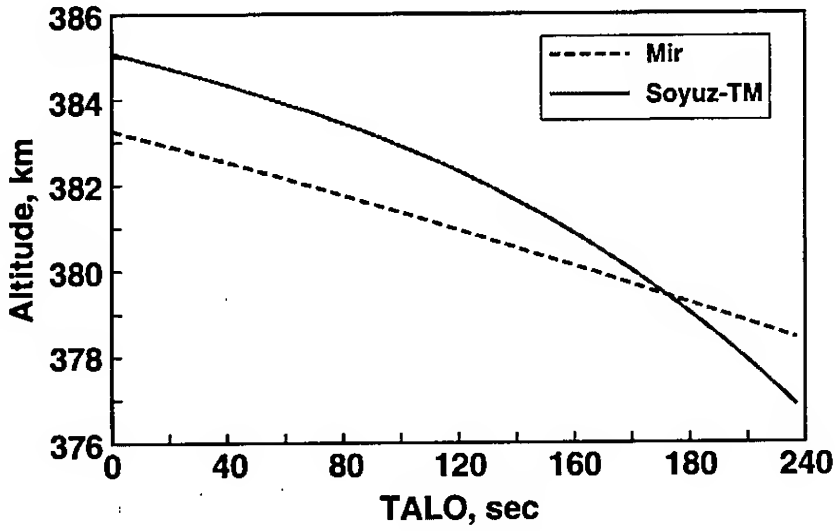

a. Spacecraft altitudes

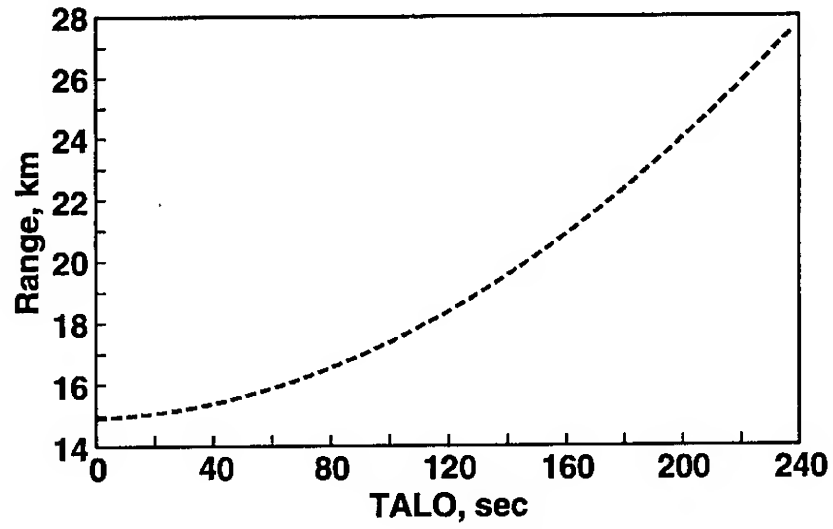

b. Range from Mir to Soyuz-TM

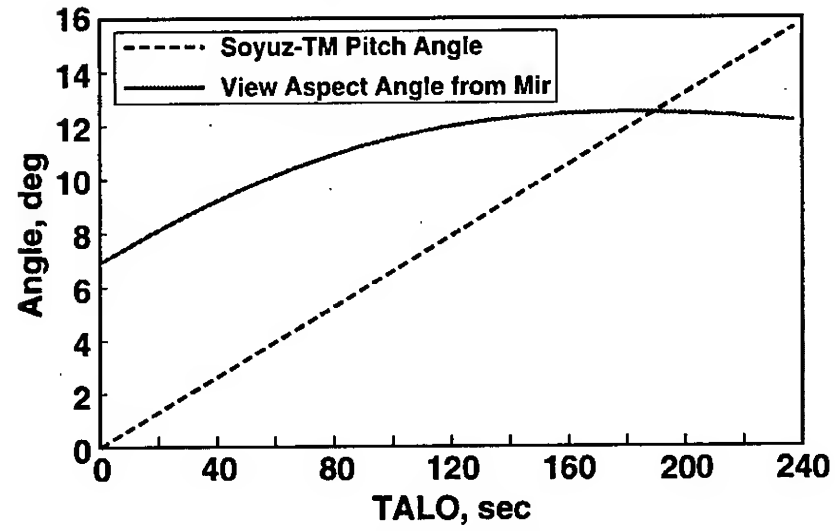

c. Soyuz-TM pitch angle and view aspect angle

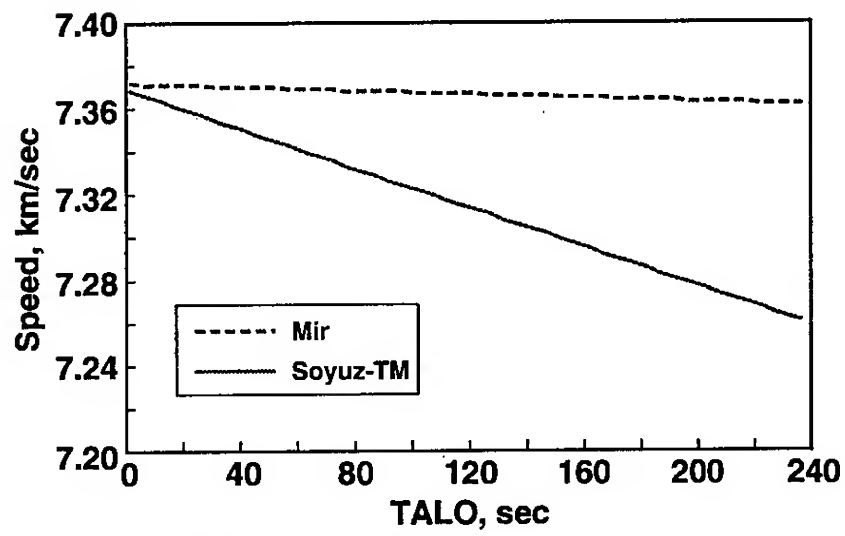

d. Mir and Soyuz-TM speeds

Figure 2. Ballistics for the August 25, 1998 Soyuz-TM re-entry braking burn.

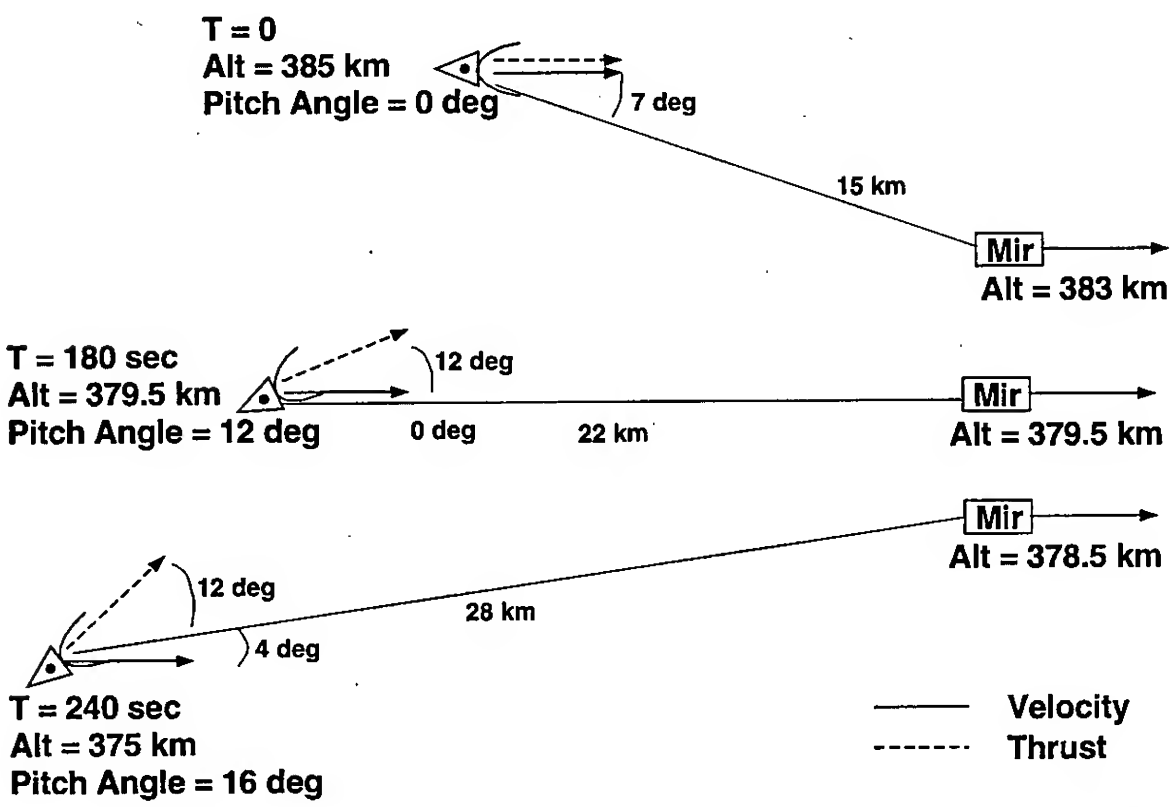

Figure 3. Schematic drawings illustrating Mir and Soyuz-TM orientations during August 25, 1998 re-entry burn.

Calibration

The calibration of the instrumentation was done in the laboratory prior to delivery to Mir and *in-situ* aboard the Mir station. The wavelength response of the Ocean Optics S2000 UV spectrometer was checked in the TsNII-MASH laboratory and found to be in keeping with the quoted manufacturer's specifications. However, it was determined that the absolute sensitivity of the spectrometer was roughly two orders lower than expected. An improved set of lenses for the fiber-optic cable were delivered to the Mir station in August 1998.

While the delivery was too late to provide spectra for the August 25, 1998 Soyuz reentry burn, calibration events using the Moon took place in October 1998. Figure 4 shows the moon spectra as measured by the UV spectrometer. Also shown are solar spectra from Frolich and London,[5] and Tousey.[6] The solar spectra have been multiplied by the Moon spectral albedo of Dobber.[7] The point to note is the excellent agreement of the MirEX spectra with the refer-

ence spectra. This agreement confirms our expectation that the Mir window has a constant transmission to wavelengths below 265 nm.

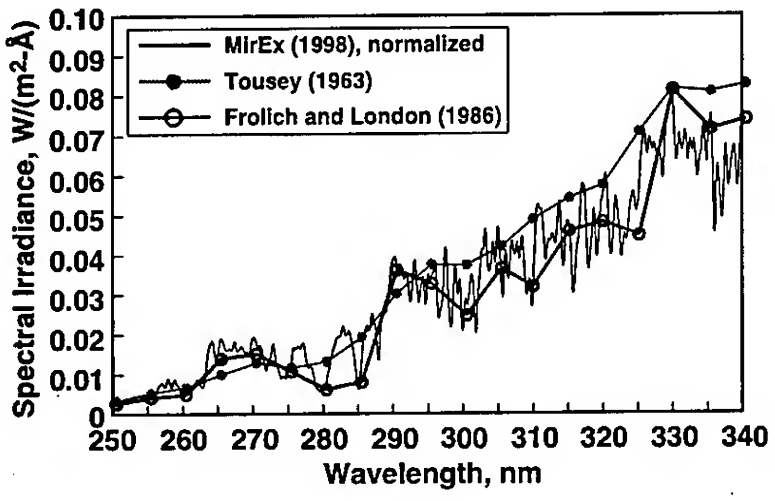

Figure 4. Moon spectrum obtained with UV spectrometer aboard Mir.

The Moon was also used for spatial calibration of the UV imager. Using the known angular dimension of the Moon as 0.5 deg as given in Ref. 7, it was determined that the UV imager field of view was 4.75 ± 0.25 deg for the May 15, 1998 Progress-M burns. The field of view of the imager collection optics for the August 25, 1998 data was roughly 1.5 times as large as that for the May 15. 1998 data. Based upon the Moon's size, as well as the distance between two stars in the imagery, it was determined on August 25, 1998 that the imager collection optics had a field of view of roughly 7.5 deg.

With the spectral measurement of the window transmission, the overall UV imager system response could be determined using the laboratory-measured response curves for the detector and the wide-band filter. The narrow-band filters were not employed for either the May 15, 1998 or August 25, 1998 data collection events. The overall UV imager response, including the Mir window, is shown in Fig. 5. The response peaks at 290 nm and falls sharply on both the short and long wavelength sides. In particular, it is essential to note that the system response to radiation at 310 nm is roughly 70 percent of the maximum, while the response at 337 nm (the wavelength for NH(A-X) emission) is roughly 15 percent of the maximum. Thus, the imager is nearly five times more sensitive to OH(A-X) emission than NH(A-X) emission.

The UV imagery was digitized using a standard 8-bit video digitizer, with careful control of the lin-

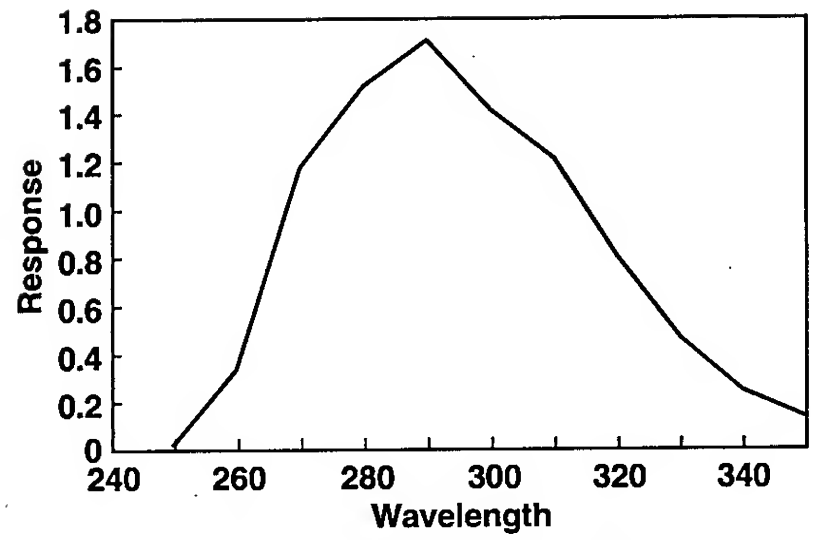

Figure 5. UV imager spectral response curve with wide band filter.

earity in order to preserve the radiometric value of the data. The absolute radiometric calibration of the UV imager was accomplished using the star θ-Oph. During the August 25, 1998 experiment, this star was located within the field of view of the imager as it recorded the plume exhaust emission, providing an excellent simultaneous calibration source. Furthermore, just prior to the August 25, 1998 experiment, the cosmonauts moved the UV camera while keeping θ-Oph within the field of view. This provided an excellent measure of the system flat field response, in which it was determined that the variation of the response across the imager was constant to within several percent.

The stellar spectra from the IUE satellite[7] were examined and found to be in agreement with other sources of spectra on θ-Oph. An absolute radiometric calibration of the data was performed. It was determined that the UV imager has sensitivity of approximately 2.1×10^{-17} W/cm^2/count at 315 nm.

A problem with the August 25, 1998 data set is that we are using a downlinked copy of the original data tape still aboard the Mir station. This downlinked version contains significant low-frequency noise due to interference. In particular, one large noise component had a well-defined period of 10 sec and appeared as a wide, low-intensity, horizontal bar across the image. To compensate for this, the plume radiation from each frame was normalized by the measured θ-Oph radiation in that frame. This 0.1-Hz noise variation will limit the absolute accuracy of this data set. Of course, once the original data tapes are returned to Earth in March 1999, the imagery will be re-digitized, and it is expected that this noise component will be eliminated.

Results

The dV3 burn was placed ideally for a measurement of the PME plume close to the nozzle exit plane. However, neither the imagery nor the spectra show any indication of emission from the plume.

The second dedicated burn, dV4, occurred at a distance of 9.2 km from Mir, with the UV imager viewing a 800-m-diam. region centered 1.6 km downstream of the nozzle exit. The imager detected a weak but definite signal corresponding to the dV4 burn. The detected radiation was spread across the entire image. The UV spectrometer field of view was slightly less than the imager, and co-aligned with the imager. No discernable signal was detected in the spectrometer for the dV4 burn.

The lack of detected spectra in the dV3 and dV4 burns is an indication that the spectrometer lacked sufficient sensitivity. This was the primary reason for sending new optics to the Mir station in August. More interesting is the lack of imagery in dV3, while the dV4 plume was detected. Two key experimental differences exist between dV3 and dV4: the angle of attack, or, in this case, the pitch angle of the PME, and the axial location of the imager field of view.

A typical raw frame of imagery from the August 25, 1998 experiment is shown in Fig. 6. The star θ-Oph is apparent near the center of the image, while the Soyuz-TM near-field plume is seen in the lower left corner. The other white pixels are instrument artifacts. A second star is in the image to the right of θ-Oph, but it is too weak to detect in a single frame image.

The near-field plume shown in Fig. 6 is spatially resolved, extending over ~10 pixels HWHM in horizontal direction and ~20 pixels HWHM in vertical direction. In comparison, the size of the star θ-Oph is 7 pixels HWHM, indicating the extent of the point spread function of the imager. There is a small "tail" of the near-field plume that extends toward the bottom of the image. This is interesting because the view aspect of the plume from the Mir station is such that the plume extends "overhead," so to speak, as depicted in Fig. 3.

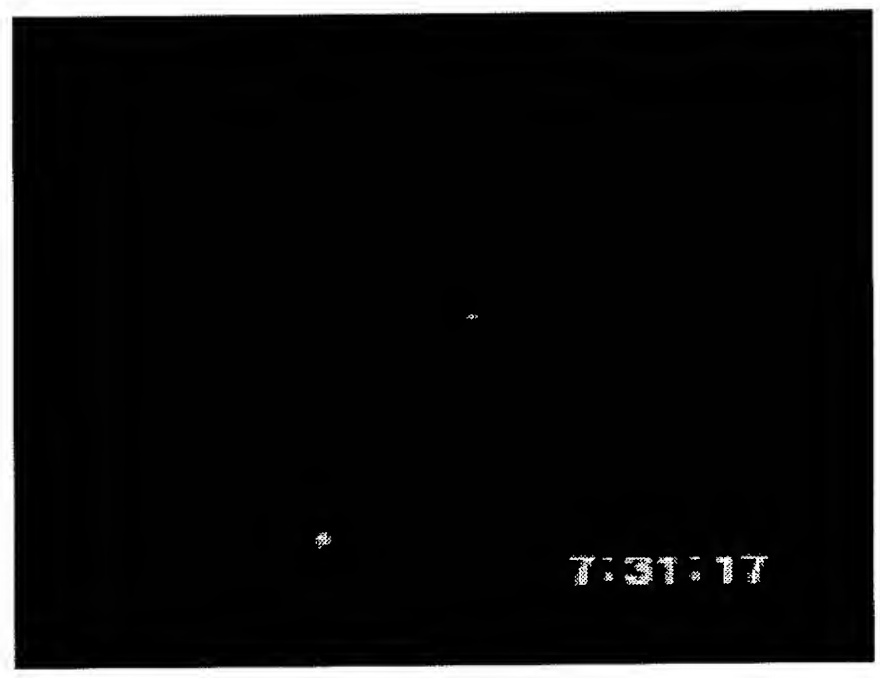

Figure 6. Single frame of August 25, 1998 Soyuz-TM reentry burn.

In addition to the near-field plume, there is a large-scale plume emission which extends over the entire active field of view of the imager. This is shown in Fig. 7, which is a processed 1-sec average taken 4 sec after ignition. In the processing, the bright near field has been masked out, and the plume motion has been removed with a tracking algorithm. The movement of the plume across the image is slow and steady, such that tracking the bright near-field plume was not a difficult task. By removing the very bright near field radiation, the far-field glow is readily apparent as a smoothly varying function across the entire active region. Note that this illumination occupies only a circular portion of the image. This is due to the instrument configuration, in which the ultraviolet image intensifier (circular geometry) is viewed by a standard rectangular CCD detector. After considerable

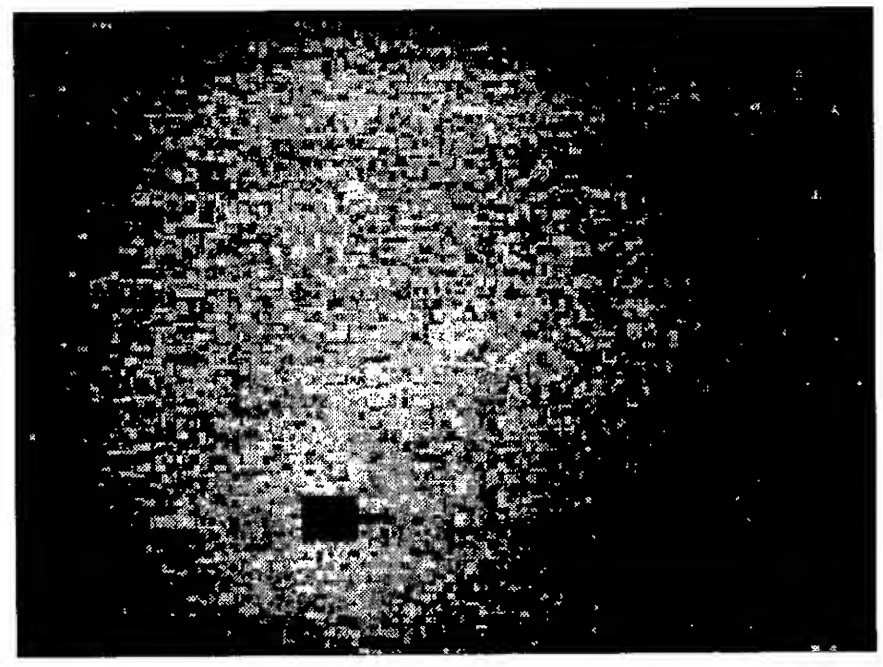

Figure 7. A 1-sec average of August 25, 1998 Soyuz-TM reentry burn shortly after ignition.

investigation, it has been determined that this far-field illumination is not due to instrument artifacts or response to the bright pixels of the near field. This glow is the result of radiation emanating from spatial locations removed from the proximity of the Soyuz-TM spacecraft. Comparing the data shown in Figs. 6 and 7, one can easily discern that there is a large difference in the relative intensity of the near and far-field radiation. For example, the near-field radiation is typically at the level of 160 counts above the noise level, while the far-field radiation signal strength is typically 2-3 counts above the noise level.

Considerable study was given to the time variation of the near-field and far-field glow intensities. Spatial summations of portions of the imagery were carried out after the imagery had been processed to remove the background level. The near-field plume intensity summation was taken as a 21 × 21 pixel region surrounding the brightest pixel in the image, and disregarding any noisy pixels and the star radiation from θ-Oph. The far-field plume intensity was calculated in two ways. The first method was to perform the summation of intensity over all pixels within the active region of the image. In this fashion, the best approximation of the total plume irradiance could be obtained. The second far-field plume intensity was computed using a 21 × 21 pixel box, at a sufficiently far distance away from the brightest pixel such that the near-field plume was not contributing to the sum. Given the dramatic difference on the pixel intensity levels, this was straightforward. The three time profiles of intensity were then smoothed with a 3-second running average.

The results of the spatial summations involving the 21 × 21 pixel subregions are shown in Fig. 8 as a plot of relative intensity as a function of time. The data in this plot cover the entire 244-sec of engine operation for the reentry burn. While the data show evidence of the low-frequency noise mentioned above, the trends are quite evident. The plume intensity from far-field region is seen to have a constant intensity over the entire burn. This fact is replicated in the time behavior of the summed intensity over the entire active region and the 21 × 21 pixel subregion profile is a good representation of the far-field plume behavior. The near-field plume intensity behaves quite differently and shows a decline in intensity as a function of time. Since the Soyuz-TM and Mir spacecraft are separating, as shown in Fig 2b, the inverse square of the range is also shown in Fig. 8. It can be seen that while the scaled range function is a fair fit to the data in the first half of the burn, the near-field data does not fall-off as fast as the scaled range function. Also notable in the near-field time profile is the significant "overshoot" of the intensity from ignition until roughly 15-20 seconds.

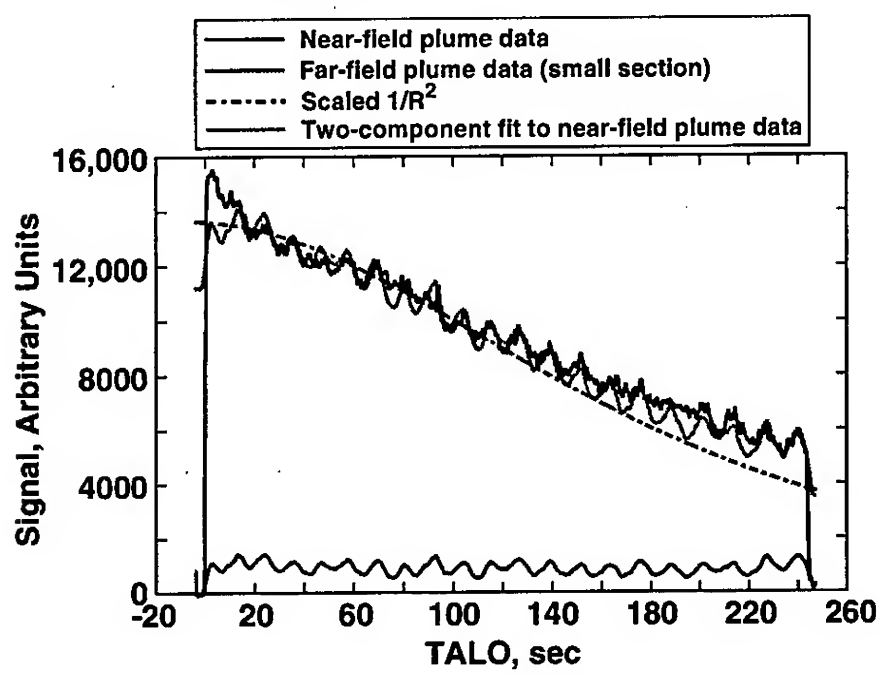

Figure 8. Time dependence of near-field and far-field plume radiation.

With the exception of the first 10 seconds, the time history of the near-field radiation can be well explained by considering the signal as a sum of a constant emission and a portion depending upon the inverse square of the range. In Fig 8, a plot of the scaling function R^{-2} is shown to illustrate the fact that the near field radiation does not decay as fast as R^{-2}. One way to account for this slow decay rate is to consider the near-field signal as a sum of radiation from the PME near-field plume along with the far-field radiation which exists along the line of sight to the PME. Upon choosing the appropriate constants to determine the ratio of contributions, the near-field data can be fit extremely well as shown in Fig 8 (red curve).

An interesting aspect of the near-field vs. far-field plume is the apparent induction time demonstrated by the far-field plume at ignition. Figure 9 shows the time history of the intensity of the two plume regions, taken for the near field of August 25, 1998, the far field of August 25, 1998, and the far field of May 15, 1998. Note that in this figure,

the intensity curves have not been temporally smoothed, as was done in Fig. 8.

In Fig. 9, one clearly sees the immediate rise in intensity observed in the near-field plume. By contrast the far-field plumes observed on May 15, 1998 and August 25, 1998 both show an identically sluggish rise in intensity. The rise in the far-field data can be fit with an expression *(1-exp(-t/τ))*, with the time constant equal to 0.5 sec. After inquiring with the manufacturer of the motor, there is no operational reason for such a slow rise time. The flow time across the UV image was also considered, but in the case of the May 15, 1998 data, the flow should fill the imager FOV in under 0.25 sec. More importantly the immediate rise of the near-field radiation shows that the PME has a rapid engine startup.

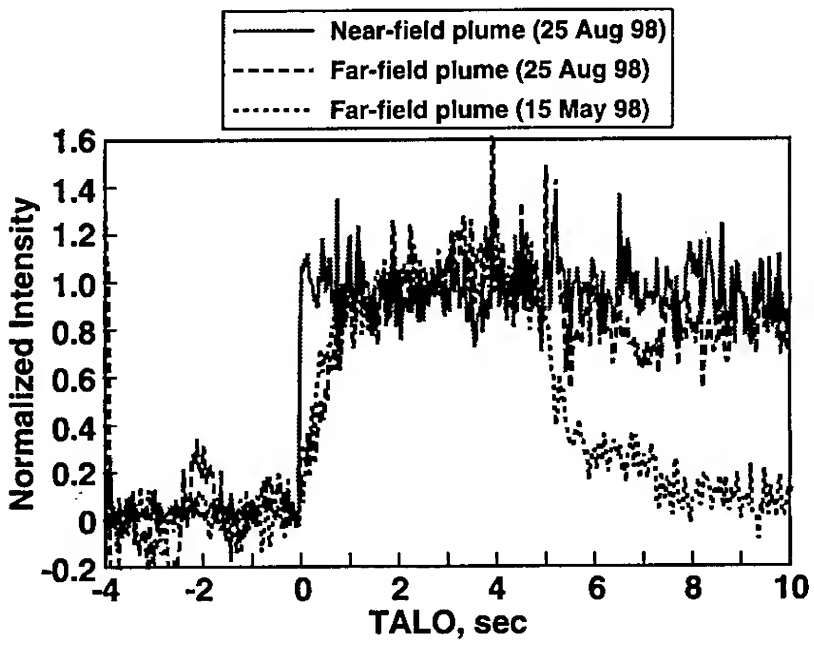

Figure 9. Induction time for far-field plume.

Furthermore, this same sluggish behavior is observed on the motor shutdown, as is displayed in the May 15, 1998 data. However, there may or may not be operational reasons for an intensity tail-off at shutdown and this needs further investigation.

Finally, using the irradiance calibration of θ-Oph, it was possible to estimate the absolute level of radiation emitted by the near- and far-field plumes. The estimates are given in Table 4 without uncertainties since the complete PME plume was not observed and it would be impossible to estimate the radiation portion outside the field of view.

The difference in the far-field plume irradiance measured on May 15, 1998 and on August 25, 1998 may be a result of the very different viewing

Table 4. PME Plume Irradiance Measurements

Date	Irradiance, W/sr
15 May 98 – Far	≥ 2.6
25 Aug 98 – Near	≥ 0.65
25 Aug 98 – Far	≥ 14

geometries, i.e., on May 15, 1998 the plume was viewed at 90-deg aspect, while on August 25, 1998 the plume was viewed nearly tail-on. Furthermore, the May 15, 1998 observation incorporated a different portion of the plume than the August 25, 1998 measurement.

Discussion

The objective of this work was to acquire ultraviolet data of near- and far-field plumes of amine propellant rocket motors in rarefied atmospheres. The data from the August 25, 1998 experiment clearly display such radiation and demarcate near- and far-field plumes, as the intensity difference between the two spatial regions is greater than a factor of ten. Careful review of these data has confirmed that the low-level signal in the far-field is indeed plume radiation and not an instrumentation artifact. In general, it has been found from both the May 15, 1998 and the August 25, 1998 experiments that the plume radiation in the bandpass of the UV imager extends over several kilometers.

The data acquired during the August 25, 1998 reentry burn represent a rare opportunity to acquire data as a continuous function of the spacecraft flight ballistic variables, as opposed to the short duration burns typified by the May 15, 1998 experiment and the referenced experiments. In addition, the simultaneous observation of the star θ-Oph within the field of view provided an excellent in-situ calibration source. With this star, the near-field radiation and a lower bound of the far-field radiation were quantified. It is to be noted that the near-field radiation intensity is in reasonable agreement with that reported by the authors from previous measurements of the PME reentry burn given the variations in experimental conditions.[3] The detection and verification of the far-field plume emission is a clear step forward from the previous efforts. While the total far-field plume radiation cannot be stated

because the plume glow extended beyond the imager field of view, a lower bound of 14 W/sr to the total radiation was made. Although not shown explicitly, the spatial distribution of the radiation from the Aug 25, 1998 observation was examined as a function of time. The analysis indicated that the far field radiation spatial profile was roughly constant in time. This combined information of intensity and spatial distribution will make possible future evaluations of the cross section energy threshhold.

The induction period of the far-field plume remains a bit of a mystery. Had the induction period not been observed on two different measurements, it would have been easy to dismiss this as a spurious instrumentation artifact, or due to the geometry of the viewpoint. The induction period is not due to geometrical effects, such as filling the field of view of the sensor with plume exhaust gas, nor is it due to a sluggish performance parameter in the PME itself, as the time scale for motor operations is on the order of tens of milliseconds. Time-dependent modeling of the system may lead to the correct explanation out of the myriad of possibilities and suggestions. It is left as a future effort to conduct that modeling.

It is possible to crudely estimate the number of reactive collisions producing the measured August 25, 1998 far-field radiation. The spatially integrated far-field power is roughly 180 W, or equivalently, a photon production rate of 3×10^{20} photons/sec. The calculations of the PME combustion predict a molecular efflux of 10^{25} H_2O molecules/sec, which indicates a photon conversion of 1 photon per every 3×10^4 expelled H_2O molecules.

Experimentally, the measurement of the camera response should satisfy any questions of the emitter identity. Ideally, future experiments should apply the narrowband filter to verify that the NH does not contribute a significant level of radiation to these data.

In the absence of far-field plume spectra, the assignment of the radiation as OH(A-X) and not NH(A-X) is based upon a comparison of these results with that of Viereck, et al.[2] The present result has a a lower bound of 180 W for the observed portion of the plume, ad compared to the 700 W of NH(A-X) radiation reported by Viereck, et al.[2] over a much larger spatial footprint of the shuttle.

There are three reasons that suggest the identity of the present emission as OH(A-X). The first is that the imager is 5 times more sensitive to OH(A-X) than NX(A-X). The second is that the Progress-M verses UDMH, while the Shuttle us MMH. Laboratory measurements by Orient, et al.[9] indicate that the NH(A-X) radiation from O-atoms colliding with (1,1)DMH is 3 times less than for MMH. Finally, the shuttle measurement of Viereck, et al.[2] was at 290 km altitude, while the Progress-M measurements occurred at 380 km altitude, resulting in 3 to 5 times less O-atom density for the Progress M-measurements. Assuming the present radiation was NH(A-X) rather than OH(A-X), and applying these three scaling factors, the absolute power level would be about an order of magnitude higher than the expected result, based upon a scaling of the value cited by Viereck, et al.[2]

The fact that it was possible to maneuver the Progress-M within the proximity of the Mir station will enable the acquisition of further data that will address some of these questions. In addition, the future acquisition of plume UV spectra will provide valuable information on the spatial distribution of key emitters.

Acknowledgements

The authors wish to recognize Dr. D. Daniel, Executive Director of the U. S. Air Force Research Laboratory (AFRL) and Dr. J. Janni of the USAFRL Office of Scientific Research (AFOSR) for their support of this effort. We would like to thank Dr. N. Anfimov for his continuous interest in this work and his efficient support of the project and B. Khmelinin for his assistance with the instrument calibration.

References

1. Viereck, R. A., Murad, E., Pike, C. P., Mende, S. B., Swenson, G. A., Elgin, J. B., Bernstein, L. S., and Lucid, S., "O(^{1}S) 557.7 nm and O(^{1}D) 630 nm Emissions in Shuttle Thruster Plumes." *J. Geophys. Res.*, Vol. 100, 1995, p. 5819.

2. Viereck, R. A., Murad, E., Knecht, D. J., Pike, C. P., Bernstein, L. S., Elgin, J. B., and Broadfoot, A. L., "The Interaction of the Atmosphere with the Space Shuttle Thruster Plume: The NH(A-X) 336-nm Emission." *J. Geophys. Res.*, Vol. 101, 1996, p. 5371.

3. Karabadzhak, G. F., Plastinin, Yu., Khmelinin, B., Teslenko, V., Shvets, N., Drakes, J. A., Swann, D. G., and McGregor, W. K., "Experimentation Using the Mir Station as a Space Laboratory," AIAA Paper 98-0288, 36th Aerospace Sciences Meeting & Exhibit, Reno NV, January1998.

4. Drakes, J. A., Swann, D. G., Karabadzhak, G. F., and Plastinin, Yu., "DSMC Computations of Progress-M Supply Spacecraft Retrofiring Exhaust Plume." 37th Aerospace Sciences Meeting & Exhibit, Reno, NV, January 1999.

5. Frolich, C. and London, J. (eds), *Revised Instruction Manual on Radiometric Instruments and Measurements*. World Climate Research Program (WCRP) Publication Series No. 7, World Meteorrological Organization/TD No. 149, Geneva, 1986.

6. Tousey, R., *Space Science Review.*, Vol. 2, 1963, p. 3.

7. Dobber, M. R., "Moon Observations with GOME." *SPIE*, Vol. 2831, 1996, p. 154.

8. Pickles, A. J., et al., *Publ. Astron. Soc. Pacific*, Vol. 110, 1998, p. 863 (http://adc.gsfc.nasa.gov/adc-cgi/caat.pl?/journal_tables/PASP/110/863/).

9. Orient, A. J. , Chutjian, A., and Murad, E., *J Chem Phys*, Vol. 101, 1995, p. 8297.